



# Study on the performance assessment of a novel hybrid heat pump system modified with dedicated mechanical sub-cooler for domestic heating applications

Shah Rukh Jamil<sup>1</sup> · Limin Wang<sup>1</sup> · Hafiz Shakeeb Arslan<sup>1</sup> · Defu Che<sup>1</sup>

Received: 13 April 2021 / Accepted: 22 July 2021 / Published online: 13 September 2021  
© Akadémiai Kiadó, Budapest, Hungary 2021

## Abstract

This article investigates the performance of a novel hybrid heat pump system, which is developed to recover the waste heat from the flue gas of domestic heating boiler. The purpose of proposed system is: to increase the return water temperature, to heat the boiler supply air, and to provide the hot air for indoor heating. The developed system consists of an air heater (acts as a dedicated mechanical sub-cooler), a multistage condensing economizer and a vapor compression heat pump. A test case of common building is considered for the performance assessment of system, which is based on the 4E analysis. For this purpose, ten refrigerants are selected. The results show that about 25.58% increase in the coefficient of performance can be obtained for the proposed model as compared to simple vapor compression cycle if operated with R245fa, which also have a lowest exergy destruction rate (38.27%) as compared to other studied refrigerants. From the perspective of improvement in boiler's energy and exergy efficiency, R114 is used to be the most effective among other refrigerant (10.33% increase in energy efficiency and 4.74% increase in exergy efficiency). Parametric study results have shown that the variation in ambient conditions should be considered carefully while selecting a refrigerant to significantly improve the system performance, exergy efficiency, and relevant economics on regional basis. From the obtained results, a novel yet simple refrigerant selection approach is proposed which can also be adopted for other thermodynamic cycles.

**Keywords** Waste heat recovery · Heat pump · Dedicated mechanical sub-cooler (DMS) · Refrigerant selection · Natural gas boiler · Performance analysis

## Nomenclature

$A$	Heat transfer area, m <sup>2</sup>
$ALR$	Annual leakage rate, % of $RC$
$AAD$	Average absolute deviation, %
$B$	Fuel saved, kg
$BCRA$	Benefit-to-cost ratio analysis
$C_p$	Specific heat, kJ kg <sup>-1</sup> K <sup>-1</sup>
$COP$	Coefficient of performance
$C$	Penalty cost, \$ ton <sup>-1</sup>
$D$	Tube diameter, m
$D_p$	Depletion number
$\dot{E}$	Exergy, kW
$EOL$	End of life leakage, % of $RC$

$F$	Fouling factor, m <sup>2</sup> ·K kW <sup>-1</sup>
$f$	Frictional factor
$H$	Humidity, kg of water vapor per kg of dry fly gas
$h$	Specific enthalpy, kJ kg <sup>-1</sup>
$h_{if}, h_{of}$	Heat transfer coefficient inside and outside the tubes, kW m <sup>-2</sup> K <sup>-1</sup>
$i$	Irreversibility, kW
$K$	Thermal conductivity, kW m <sup>-1</sup> K <sup>-1</sup>
$LHV$	Lower heating value, kJ Nm <sup>-3</sup>
$LT$	System lifetime, years
$M$	Molar mass, kg kmol <sup>-1</sup>
$m$	Mass, kg Nm <sup>-3</sup> of fuel)
$\dot{m}$	Mass flow rate, kg s <sup>-1</sup>
$M_{emissions}$	Mass equivalent to emissions, kg
$N$	Fuel consumption, kg
$Nu$	Nusselt number
$P$	Pressure, Pa
$Pr$	Prandtl number
$\dot{Q}$	Heat transfer rate, kW

✉ Defu Che  
dfche@mail.xjtu.edu.cn

<sup>1</sup> State Key Laboratory of Multiphase Flow in Power Engineering, School of Energy and Power Engineering, Xi'an Jiaotong University, Xi'an 710049, People's Republic of China

$Re$	Reynolds number
$RC$	Refrigerant charge, kg
$s$	Specific entropy, $\text{kJ kg}^{-1} \text{K}^{-1}$
$SI$	Sustainability index
$T$	Ambient temperature, $^{\circ}\text{C}$
$t$	Time, hours
$U$	Overall heat transfer coefficient, $\text{kW m}^{-2} \text{K}^{-1}$ )
$\dot{V}$	Volume flow rate, $\text{m}^3 \text{s}^{-1}$
$\dot{W}$	Power, kW
$x$	Mass fraction, %
$\dot{x}$	Exergy destruction, kW
$Z$	Total penalty cost saved, \$

### Greek symbols

$\varphi$	Relative humidity
$\Delta T$	Temperature difference, $^{\circ}\text{C}$
$\eta$	Efficiency, %
$\mu$	Emission factor

### Subscripts

A	Ambient
cw	Condensed water
dg	Dry flue gas
dp	Dew point
If	Inside flow
O	Reference or dead state
of	Outside flow
op	Operating
P	Partial
ref	Refrigerant
s	Saturated
sl	Surface losses
T	Total
wv	Water vapor
w	Water
wo	Water leaving the boiler
wi	Water entering the boiler

### Abbreviations

AH	Air heater
Aux	Auxiliaries
B	Blower
CEPCI	Chemical Engineering Plant Cost Index
COMP	Compressor
COND	Condenser
C	Chimney
EVAP	Evaporator
FG	Flue gas
GWP	Global warming potential
HA	Hot air
IDCCU	Indirect contact condensing unit
LHV	Lower heating value
LMTD	Logarithmic mean temperature difference
NG	Natural gas

ODP	Ozone depletion potential
RW	Return water
SA	Supply air
SW	Supply water
WHR	Waste heat recovery

## Introduction

In recent times, the human urbanization is paced up rapidly, which enforced the construction of more residential areas. Due to this upsurge in the construction of more and more residential sectors, the use of the state-of-art technologies for human comfort has also attained the serious attention. More specifically, these technologies are being adopted for the provision of thermal comfort. The use of boilers for the domestic heating is common, which is further increasing over the time as well. The unwanted emissions and waste heat from the boiler are the major concerns of the current century. Waste heat and harmful emissions are released in to the atmosphere due to the combustion of fossil fuels, which are responsible for the increase in global warming and have a direct impact on the depletion of ozone layer [1]. The growth in global warming is the cause of severe climate change. In return, the climate change may have adverse effects on the climatic conditions, livestock, agriculture, and forests [2]. These emissions also cause health diseases such as cancer, eye infections, asthma, tuberculosis (TB), and lung infections [3]. These factors have given rise to questions toward the energy security and environmental sustainability on global scale with a much-needed solution. By considering the above-discussed issues, this research work is focused on providing a reasonable solution. In order to provide a better solution, we suggest the use of waste heat recovery (WHR) technologies [4] as a suitable option. Furthermore, the extract of previous studies has also vitalized the importance of these technologies by highlighting their impact on the global scale. Moreover, it is notable that the flue gas condensation can assist in recovering the waste heat and emission reduction with the adaptation of suitable WHR technology [5]. In addition to that, proper utilization of the recovered heat can be helpful in reducing the consumption of fuel and associated emissions [6]. Lastly, the reduction in carbon taxes can also be achieved significantly [7].

The use of heat pumps is a hot topic among the available technologies for waste heat recovery. Heat pumps are widely used in domestic, industrial, and transportation sectors due to their flexible design and variety of range [8]. Modification in the design of heat pumps can enhance their techno-economic performance and the desired benefits can be achieved [9]. The use of a proper working fluid can further boost the performance. Refrigerant selection should be

made on the basis of operating conditions to get the desired outcomes because of the difference in their properties [10]. If we have a look on the studies conducted by researchers, we can find the sufficient vital information on the heat pump development, integration and performance assessment by using different refrigerants. For example, in a study conducted by Cooper et al. [11], they have discussed the potential of heat pumps in energy and emission reduction for UK food and beverage industry. They concluded that the reduction in CO<sub>2</sub> emissions of around 2.6 Mt per year could be achieved. Todorović et al. [12] performed a comparative study on the use of heat pumps for heat recovery from the waste water and its provision for hot water in hotels. The study on the substitution of heat pumps for boilers is conducted by Bergamini et al. [13]; they employed three different heat pump cycles and compared their performance with the boiler for heat production by focusing on the *COP* and exergy efficiency. They concluded that the use of heat pumps for heat delivery up to 180 °C is competitive for boiler substitution. Mateu-Royo et al. [14] proposed an integration of heat pump in to a district heating network (DHN) by using low-GWP refrigerants and yielded that about 47% reduction in CO<sub>2</sub> emissions can be achieve. Deymi-Dashtebayaz et al. [15] studied the potential of HFC working fluids for ground source heat pump developed for residential heating applications. Bamigbetan [16] developed a hydrocarbon heat pump for waste heat recovery with a potential of temperature lift of about 58–72 K. A theoretical investigation is presented by Song et al. [17] on the cascade heat pumps for space heating by using refrigerants R134a and R744. Ma et al. [18] performed an experimental study to analyze the performance of a cascade heat pump water heater system by employing different zeotropic refrigerants. D'Agaro [19] simulated a commercial heat pump system integrated with R134a/R744 cascade system for the supermarket heating by using refrigerants R744 and R404A. Mota-Babiloni [20] conducted an optimization based study for HTHP cascades by using low-GWP refrigerants; as a result, maximum *COP* of 3.15 was obtained by the pair of pentane/butane. According to Fukuda [21], R1234ze(Z) is the suitable working fluid as compared to R123ze(E) for the heat pumps used in industrial applications. Ambient conditions can also fluctuate the performance of heat pumps greatly, and the research conducted by Maddah and Safaei [22] is very significant in this regard to determine the optimal discharge pressures for maximum performance in transcritical CO<sub>2</sub> heat pump cycles. By extending the discussion further, Urbanucci et al. [23] performed a thermo-economic analysis on the heat pumps integration in tri-generation systems. According to them, 10.3% and 10.6% savings achieved as compared to traditional tri-generation and cogeneration systems, respectively. Ambient conditions have a great impact on the performance of heat pumps. Pitarch et al. [24] analyzed the components of heat pump

by using exergy method on the basis of external conditions. They concluded that most of exergy destruction occurs in condenser due to the variation in inlet fluid temperature. In these days, the integration of heat pumps with renewable energy-based cogeneration systems is very popular in terms of performance and economics [25], while the use of evolutionary algorithms for the exergo-economic optimization of thermal systems can also be very helpful because of their tendency to achieve more reliable results [26]. Some researchers also suggest the use of nano-fluids as a working medium for the heat pumps due to their efficient heat transfer capabilities [27, 28]. In addition to that, the use of heat pipes can also be a good option, while the use of different nano-fluids, such as ZnO [29] and other hybrid nano-fluids [30, 31], can also enhance the performance, which is largely dependent on their thermophysical properties [32, 33]. Their coupling for domestic heating purposes can be a good topic of further research. Conclusively, on the basis of existing literature it can be said that the heat pump integration is a better solution to recover the waste heat.

Now, if we talk about the performance assessment, energy, exergy, economic and environmental analysis (4E) are the main determinant factors in the design, modeling and optimization of thermal systems. The implementation of these parameters can be witnessed through many research studies. Xu et al. [34] performed a comparative study between two absorption-compression cycles on the basis of 4E analyses to select the suitable operating mode. 4E analyses were performed by Liu et al. [35] on an organic Rankine cycle (ORC) and absorption heat pump-based hybrid system to capture and store the CO<sub>2</sub> from the coal chemical industry. Deymi-Dashtebayaz [36] proposed an air source heat pump for data center cooling, the results yielded in 35,000 m<sup>3</sup> of fuel, 20.8 MW electricity, and 121 tons CO<sub>2</sub> savings on annual basis. Maddah [37] conducted a comparative study between different types of industrial wastewater heat pumps and obtained the highest *COP* of 5.104. Jain et al. [38] studied different configurations for a 170 kW chiller to select the suitable one on the basis of 4E analyses. Liu and Dai [39] conducted the 4E analysis on a CO<sub>2</sub> based heat pump system with a purpose of residential heating (China). They concluded that the use of heat pumps is more feasible as compared to fuel fired boilers. Maddah et al. [40] performed a comparative study on air and geothermal source heat pump cycles (operated with different refrigerants) through 4E analysis and concluded that R134a can be a best suitable option among the other studied refrigerants. Dadsetani et al. [41] conducted an exergo-economic optimization on Linde–Hampson gas liquefying cycles for argon. From these studies, the importance of 4E analysis can be well judged.

Although the importance of heat pumps cannot be denied due to their positive role in energy security and

environmental sustainability on global scale, there are some research gaps related to the integration of heat pumps in domestic heating networks, which are need to be addressed. The main points of consideration are: (a) due to high return water temperature, it is challenging to extract the maximum possible heat from the flue gas, (b) sufficient amount of heat is wasted in the vapor compression cycle during the expansion stage, (c) for residential areas with relatively larger heating requirements, the research on the coupling of waste heat-driven heat pumps is still lacking, and lastly (d) there is a need of working fluid selection approach that can produce more reliable and simple results by focusing on the energy security, environmental sustainability and economic feasibility. By focusing on the above highlighted issues, in this work, a hybrid heat pump system with dedicated mechanical sub-cooler (DMS) is proposed with an objective of performance improvement by minimizing the internal heat loss and reduced costs. Unlike other researches, in which the heat recovered by dedicated mechanical sub-cooler (DMS) is utilized in another heat pump cycle, an air heater is introduced as a sub-cooler. The problem with the heat pump cycles driven by the captured heat of DMS is the addition of a new cycle (plant cost) and relevant operating cost (including the maintenance cost), which is eliminated in this work by efficiently utilizing the captured heat for increasing the temperature of boiler supply air, while the remaining heat can be provided to heating area. The proposed system can significantly contribute in the ongoing research on waste heat recovery technologies by focusing on the elimination of internal heat loss issues of thermodynamic cycles. The proposed system is coupled with a test case having larger heating area requirements. To study the performance of developed system, 10 refrigerants are selected. A comprehensive thermodynamic, economic, environmental and sustainability analysis is performed. Parametric analysis is conducted to study the effect of ambient conditions on the performance and economics of the system. Lastly, a novel yet simple technique is proposed for the selection of suitable working fluid for thermodynamic cycles.

## Model formulation

This paper presents a hybrid heat pump system to recover the maximum waste heat from the flue gas with an effective utilization technique (Fig. 1). The model consists of an air heater, a vapor compression heat pump, and a multistage indirect contact condensation economizer. Flue gas (1) enters the first stage of indirect contact condensation unit (IDCCU), which is the evaporator of heat pump. Evaporator condenses the flue gas with the help of refrigerant (5). After leaving the evaporator, flue gas enters the air heater (AH-1) (2). At this stage, ambient air (10)

is introduced to enhance the condensation and to capture the residual heat of the flue gas. The heated air (11) is then used for indoor heating purposes. The refrigerant leaving the evaporator enters the compressor (6), and its pressure increases. The refrigerant transfers heat to the return water (14) in the condenser. At the outlet of the condenser, some heat is present in the refrigerant (8) due to the high return water temperature. At this stage, an air heater (AH-2 or DMS) is introduced to capture the remaining heat of the refrigerant. The heat captured at this stage (13) is used as boiler air supply and for indoor heating. The system has the following advantages:

- Enhanced heat and condensate recovery from the flue gas with a step toward environmental sustainability and energy security.
- Provision of hot air for indoor heating without additional costs.
- Increased boiler air supply temperature can increase boiler efficiency and reduce fuel cost
- Reduction in the internal heat losses of heat pump as compared to conventional configuration.
- System configuration can be modified as needed respective to the type of process.

## Refrigerant selection

Heat pump performance mainly depends on the selection of an appropriate working fluid. When evaluating refrigerants, many aspects must be considered. In order to be suitable for

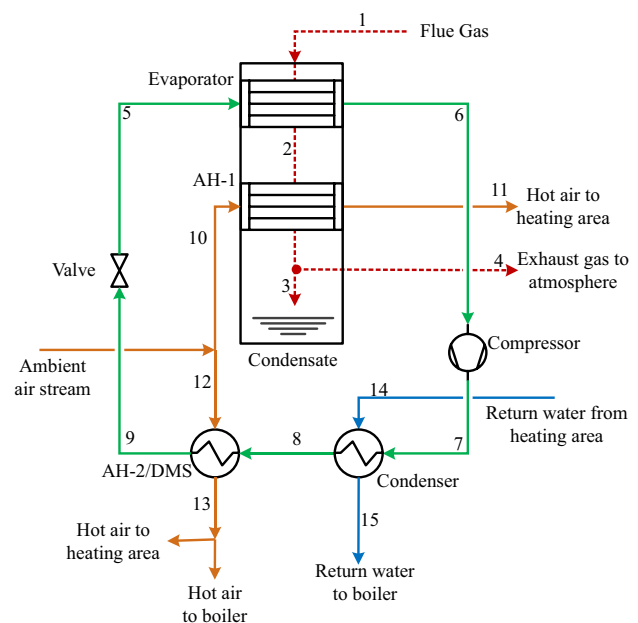


Fig. 1 Schematic diagram of the proposed hybrid heat pump system

operation in heat pumps, fluids, whether pure or mixed, must comply with certain requirements, such as chemical properties, thermodynamic properties, safety concerns and environmental issues. For good performance of the heat pump system, it is very important to choose the right working fluid. To this end, we have selected 10 refrigerants to observe the performance of the system proposed in this study (Table 1). The selected refrigerants are well recommended by multiple authors [42, 43].

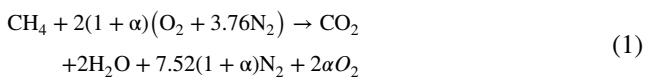
**Assumptions**

The following assumptions are taken into account while modeling the system [44, 45]:

- Ambient conditions are 3.5 °C and 1 bar;
- Steady state conditions are assumed;
- Kinetic and potential energy losses are neglected;
- Combustion in the boiler is considered as complete;
- Natural gas is considered as pure methane;
- Air composition is 79% N<sub>2</sub> and 21% O<sub>2</sub>;
- Excess air ratio is 1.05;
- Heat losses and pressure drops are ignored in system components;
- Isentropic and mechanical efficiencies for compressor, blower, and fan are taken as 0.80 and 0.99, respectively.

**Boiler model**

The combustion of fuel can be expressed by the following equation [46]:



Boiler efficiency is measured on the basis of lower heating value of fuel (36,740 kJ Nm<sup>-3</sup>) [47] by using the following equation [48]:

$$\eta_{Boiler} = \frac{\dot{m}_w \times C_{p,w} (T_{wo} - T_{wi})}{\dot{V}_{fuel} \times LHV} \tag{2}$$

**Flue gas model**

Flue gas condensation mainly depends on the dew point, which in turn depends on the partial pressure of water vapor and the humidity ratio of the gas. In this work, the flue gas condensation is based on water vapors, oxygen, nitrogen, and carbon dioxide. The humidity (*H*) of gas is calculated by [49]:

$$H = \frac{M_{wv}}{M_{dg}} \left( \frac{P_p}{P_t - P_p} \right) \tag{3}$$

Relative humidity is obtained from the following expression:

$$\varphi = \frac{P_p}{P_s} \tag{4}$$

Equation (3) is modified as:

$$H = \frac{M_{wv}}{M_{dg}} \left( \frac{\varphi P_s}{P_t - \varphi P_s} \right) \tag{5}$$

Here,  $\frac{M_{wv}}{M_{dg}}$  is:

$$\frac{M_{wv}}{M_{dg}} = \frac{M_{H_2O}}{CO_2\% M_{CO_2} + O_2\% M_{O_2} + N_2\% M_{N_2}} \tag{6}$$

Antoine’s equation is used to measure the saturated pressure of water vapors [50]:

**Table 1** List of selected refrigerants in the present study

Refrigerant	Chemical formula	Molecular mass/g mol <sup>-1</sup>	Critical temperature/°C	Critical pressure/bar	Normal boiling point/°C	ASHRAE safety group	ODP	GWP
R114	CClF <sub>2</sub> CClF <sub>2</sub>	170.9	145.7	32.6	3.8	A1	0.58	8590
R134a	CH <sub>2</sub> FCF <sub>3</sub>	102.0	101.1	40.6	-26.1	A1	0	1300
R245fa	CHF <sub>2</sub> CH <sub>2</sub> CF <sub>3</sub>	134.0	154.0	36.5	14.9	B1	0	858
R600	CH <sub>3</sub> CH <sub>2</sub> CH <sub>2</sub> CH <sub>3</sub>	58.1	152	38	-0.5	A3	0	4
R717	NH <sub>3</sub>	17.0	132.3	113.3	-33.3	B2L	0	0
R718	H <sub>2</sub> O	18.0	373.9	220.6	100.0	A1	0	0
R744	CO <sub>2</sub>	44.0	31.98	73.8	-78.4	A1	0	1
R1233zd(E)	CF <sub>3</sub> CH=CHCl(E)	130.5	166.5	36.2	18	A1	0.0034	1
R1234yf	CH <sub>3</sub> CF=CH <sub>2</sub>	114.0	94.7	33.8	-29.5	A2L	0	< 1
R1234ze(E)	CF <sub>3</sub> CH=CHF(E)	114.0	109.4	36.4	-19.0	A2L	0	< 1



$$P_s = 133.18 \exp\left(18.3036 - \frac{3816.44}{273.15 + t - 46.13}\right) \quad (7)$$

In Eq. (7), applicable range for  $t$  is 283–453 k. The combination of Eq. (5) and (7) yields the expression to calculate the wet flue gas humidity:

$$H = \left(\frac{M_{wv}}{M_{dg}}\right) \frac{133.18 \varphi \exp\left(18.3036 - \frac{3816.44}{273.15 + t - 46.13}\right)}{P_t - \left\{133.18 \varphi \exp\left(18.3036 - \frac{3816.44}{273.15 + t - 46.13}\right)\right\}} \quad (8)$$

After the modification of Eq. (8), the equation to calculate the dew point is:

$$t = \frac{3816.44}{18.3036 - \ln \frac{H \cdot P_t}{133.18 \left(H + \frac{M_{wv}}{M_{dg}}\right)}} - 227.02 \quad (9)$$

### Thermodynamic model

Thermodynamic modeling of system components is carried out based on Eqs. 10 to 14. The equations governed for the mass conservation are based on the following equation:

$$\sum \dot{m}_{in} = \sum \dot{m}_{out} \quad (10)$$

For material balance in the system streams, the following equation is considered:

$$\sum \dot{m}_{in} x_{in} = \sum \dot{m}_{out} x_{out} \quad (11)$$

Energy conservation takes place during the process can be elaborated by the following equation:

$$\sum \dot{Q} - \sum \dot{W} = \sum \dot{m}_{out} h_{out} - \sum \dot{m}_{in} h_{in} \quad (12)$$

Exergy destruction in the system is calculated through irreversibilities by following equations:

$$\dot{x}_{total} = \sum \dot{x}_i \quad (13)$$

Exergy of the streams is calculated by equation:

$$\dot{E} = \dot{m}[(h - h_0) - T_a(s - s_0)] \quad (14)$$

On the basis of the above-mentioned equations, the relevant governing equations are derived according to the schematic presented in Fig. 2 and presented in Table 2.

$COP$  of heat pump is calculated as:

$$COP_{HP} = \frac{\dot{Q}}{\dot{W}} = \frac{\text{Heat Supplied by HP}}{\text{Compressor Work}} \quad (15)$$

Heating  $COP$  is obtained from:

$$COP_{\text{Heating}} = \frac{\dot{Q}_{\text{Heating}}}{\dot{W}_{\text{Comp}} + \dot{W}_{\text{Aux}}} \quad (16)$$

Heat transfer rate in heat exchanger is calculated by [51]:

$$Q = UA\Delta T_{\text{LMTD}} \quad (17)$$

Log mean temperature difference ( $\Delta T_{\text{LMTD}}$ ) is calculated as:

$$\Delta T_{\text{LMTD}} = \frac{\Delta T_{\text{of}} - \Delta T_{\text{if}}}{\ln \frac{\Delta T_{\text{of}}}{\Delta T_{\text{if}}}} \quad (18)$$

Heat transfer coefficient ( $U$ ) is obtained from [52]:

$$U = \frac{1}{\left[\left(\frac{D_{\text{of}}}{D_{\text{if}}}\right)\left(\frac{1}{h_{\text{if}}}\right) + \left(\frac{D_{\text{of}}}{D_{\text{if}}}\right)(F_{\text{if}}) + (F_{\text{of}}) + \left(\frac{1}{h_{\text{of}}}\right)\right]} \quad (19)$$

From the above equation, the value of fouling factor is taken as  $F_{\text{if}} = F_{\text{of}} = 0.09 \text{ m}^2 \text{ K/kW}$  [53]. The value of heat transfer coefficients for inner and outer surfaces of the tubes is calculated by assuming carbon steel as a material. The following equation is used to calculate the heat transfer coefficient:

$$Nu = \frac{h \times D}{k} \quad (20)$$

In the above equation,  $Nu$  is the Nusselt Number (-),  $k$  is the thermal conductivity ( $\text{kW} \cdot \text{m}^{-1} \text{ K}^{-1}$ ), and  $D$  is the diameter of tube (m). The above equation can be further modified to obtain the heat transfer coefficient for inside and outside the tubes of heat exchanger. To calculate the Nusselt number inside the tube, the co-relation developed by Petukhov–Popov is used [54]:

$$Nu = \frac{(f/8)Re \cdot Pr}{K_1 + K_2(f/8)^{1/2}(Pr^{2/3} - 1)} \quad (21)$$

where  $Re$  is the Reynolds number (-) and  $Pr$  is the Prandtl number (-).  $K_1 = 1 + 3.4f$  and  $K_2 = 11.7 + (1.8/Pr^{1/3})$ . The valid range for Eq. 55 is:  $2300 < Re < 5 \times 10^6$  and  $0.5 < Pr < 2000$ , while  $f$  is the friction factor, which is obtained by:

$$f = [1.82 \log(Re) - 1.64]^{1/4} \quad (22)$$

In the proposed system, refrigerant flows inside the tubes in the case of evaporator, condenser, and AH-2. For the case of AH-1, air flows through the tubes. By taking the respective values of specific fluids, the heat transfer coefficient inside the tubes is calculated.

To calculate the heat transfer coefficient outside the tubes, Eq. 20 is used after some modifications. While developing

**Fig. 2** Schematic of the test case equipped with the proposed system

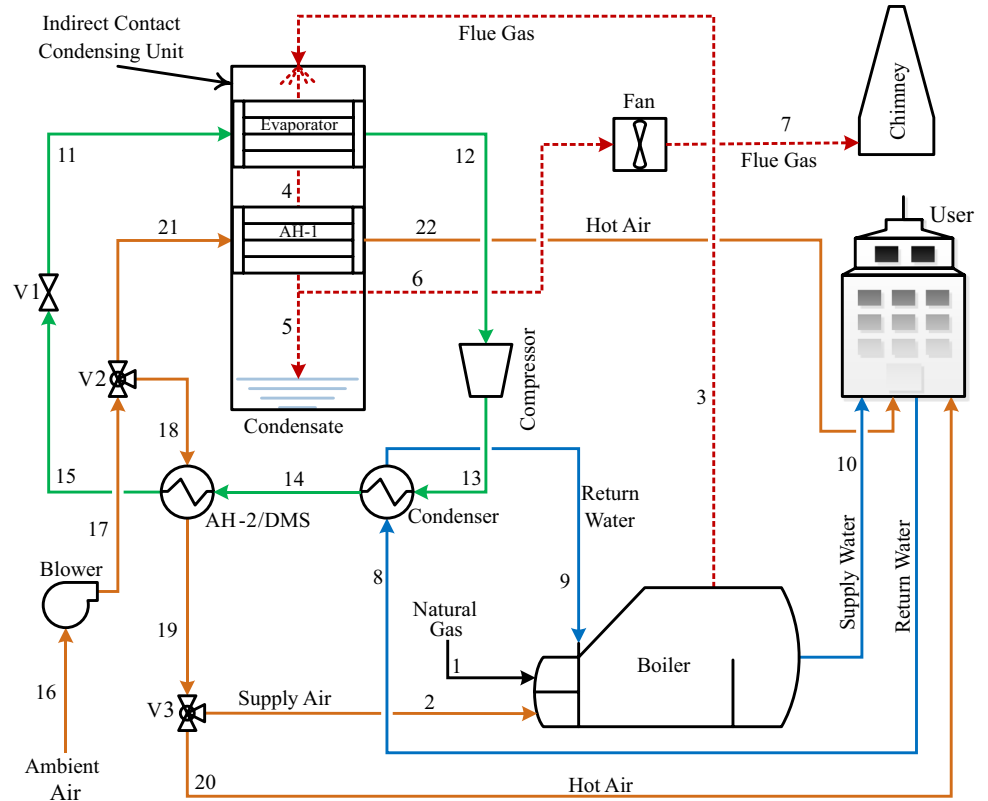


**Table 2** Equations governed for the proposed system

Component	Governing equations	Component	Governing equations
Boiler	$\dot{m}_1 + \dot{m}_2 + \dot{m}_9 = \dot{m}_3 + \dot{m}_{10}$ $\dot{E}_{fuel} + \dot{E}_{air} = \Delta \dot{E}_w + \dot{E}_{fg} + \dot{E}_{sl}$ $\dot{E}_{fuel} = \dot{m}_{fuel} \times LHV_{fuel}$ $\dot{I}_B = \dot{E}_1 + \dot{E}_2 + \dot{E}_9 - \dot{E}_3 - \dot{E}_{10}$	Evaporator	$\dot{m}_3 + \dot{m}_{11} = \dot{m}_4 + \dot{m}_{12}$ $\dot{Q}_{Evap} = \dot{m}_{ref}(h_{12} - h_{11})$ $\dot{I}_{Evap} = \dot{E}_3 + \dot{E}_{11} - \dot{E}_4 - \dot{E}_{12}$
AH-1	$\dot{m}_4 + \dot{m}_{21} = \dot{m}_5 + \dot{m}_6 + \dot{m}_{22}$ $\dot{Q}_{AH-1} = \dot{m}_{air}(h_{22} - h_{21})$ $\dot{I}_{AH-1} = \dot{E}_4 + \dot{E}_{21} - \dot{E}_5 - \dot{E}_6 - \dot{E}_{22}$	Compressor	$\dot{m}_{12} = \dot{m}_{13}$ $\dot{W}_{Comp} = \dot{m}_{ref}(h_{13} - h_{12})$ $\dot{I}_{Comp} = \dot{W}_{Comp} + \dot{E}_{12} - \dot{E}_{13}$
Condenser	$\dot{m}_{13} + \dot{m}_8 = \dot{m}_{14} + \dot{m}_9$ $\dot{Q}_{Cond} = \dot{m}_{ref}(h_{14} - h_{13})$ $\dot{I}_{Cond} = \dot{E}_{13} + \dot{E}_8 - \dot{E}_{14} - \dot{E}_9$	AH-2/DMS	$\dot{m}_{14} + \dot{m}_{18} = \dot{m}_{15} + \dot{m}_{19}$ $\dot{Q}_{AH-2} = \dot{m}_{ref}(h_{15} - h_{14})$ $\dot{I}_{AH-2} = \dot{E}_{14} + \dot{E}_{18} - \dot{E}_{15} - \dot{E}_{19}$
Valve-1	$\dot{m}_{15} = \dot{m}_{11}$ $h_{15} = h_{11}$ $\dot{I}_{V1} = \dot{E}_{15} - \dot{E}_{11}$	Blower	$\dot{m}_{16} = \dot{m}_{17}$ $\dot{W}_{Blow} = \dot{m}_{air}(h_{17} - h_{16})$ $\dot{I}_{Blow} = \dot{W}_{Blow} + \dot{E}_{16} - \dot{E}_{17}$
Valve-2	$\dot{m}_{17} = \dot{m}_{18} + \dot{m}_{21}$ $h_{17} = h_{18} = h_{21}$ $\dot{I}_{V2} = \dot{E}_{17} - \dot{E}_{18} - \dot{E}_{21}$	Fan	$\dot{m}_6 = \dot{m}_7$ $\dot{W}_{Fan} = \dot{m}_{fg}(h_7 - h_6)$ $\dot{I}_{Fan} = \dot{W}_{Fan} + \dot{E}_6 - \dot{E}_7$
Valve-3	$\dot{m}_{19} = \dot{m}_2 + \dot{m}_{20}, h_{19} = h_2 = h_{20}, \dot{I}_{V3} = \dot{E}_{19} - \dot{E}_2 - \dot{E}_{20}$		

the co-relations, the alignment of tubes is considered as in-line. The equation proposed by Dittus and Boelter for calculating the Nusselt number is used [55]:

$$Nu = 0.023Re^{0.8}Pr^n \tag{23}$$

The equation is valid for all types of fluids. The value of  $n$  can be taken as 0.3 or 0.4, respectively, for cooling

or heating. For the case of current system, this equation is modified with Eq. 20 after modification for the outer surface of tubes, which are in contact with flue gas (evaporator and AH-1), air (AH-2) and water (condenser).

### Cost model

Cost analysis is an important function that determines whether the system is acceptable or not. The cost model consists of three parameters: capital cost, operational cost, and maintenance cost. Cost of the components is calculated as [56]:

$$C_E = C_B \left( \frac{Q}{Q_B} \right)^M \tag{24}$$

where  $C_E$ ,  $C_B$ ,  $Q$ , and  $M$  are equipment cost, base cost depending on  $Q_B$ , equipment capacity and constant, respectively, depending on the equipment type. Corrected cost  $C_C$  for material  $f_M$ , pressure  $f_P$  and temperature  $f_T$  are obtained from:

$$C_C = C_B \left( \frac{Q}{Q_B} \right)^M f_M f_P f_T \tag{25}$$

Equipment cost information on the basis of correction factors is listed in Table 3.

Modified equipment cost through plant cost index method can be obtained from:

$$C_E = C_{E,2000} \frac{C_{EPCI,2020}}{C_{EPCI,2000}} \tag{26}$$

$$M_{\text{emissions, Electrical}} = (\mu_{\text{CO}_2} + \mu_{\text{SO}_2} + \mu_{\text{NO}_x}) \cdot t_{\text{op}} (\dot{W}_{\text{Comp}} + \dot{W}_{\text{Blow}} + W_{\text{Fan}}) \tag{29}$$

The operating cost on the basis of power consumed by compressor, fan, and blower is calculated as:

$$C_O = T_O \left[ \frac{C_E}{0.0036} \times (E_C + E_B + E_F) \right] \tag{27}$$

Cost values of electricity, water, fuel, and heating used in this study are given in Table 4. The average heating season is taken as 4 months. The payback period and profit are calculated based on the 24 h of operation per heating season.

Benefit-to-cost ratio analysis (*BCRA*) is a financial decision-making tool for simply analyzing project costs and related benefits. *BCRA* is different from general cost-effectiveness analysis, which only considers accounting costs. Most engineering economic and financial feasibility studies involve cost-effectiveness analysis, not benefit-to-cost ratio analysis [58]. *BCRA* determines whether the profit of the project is greater than the cost incurred during the execution of the project. Moreover, the method focuses on the monetization of revenue by considering the monetary value of each major benefit from the project (WHR in current case). This can be simply understood by the following equation:

$$BCRA = \frac{\text{Discounted value of benefits}}{\text{Discounted value of costs}} \tag{28}$$

### Environmental analysis modeling

Flue gas emissions are a major issue for environmental sustainability.  $\text{CO}_2$ ,  $\text{SO}_2$ , and  $\text{NO}_x$  are termed as the main environmental pollutants, and it is necessary to study the environmental impact of the WHR system. Additional fuel combustion is not involved in the presented WHR system. So, emissions related to electricity consumption are considered. The expression to calculate the electrical emissions is [34]:

Expression to calculate natural gas combustion emissions in boiler is [39]:

**Table 4** Prices used for cost analysis [57]

Description	Value
Electricity/\$ KWh <sup>-1</sup>	0.08
Natural gas/\$ Nm <sup>-3</sup>	0.33
Water/\$ m <sup>-3</sup>	0.64
Indoor heating/\$ m <sup>-2</sup> per month	0.82

**Table 3** WHR components cost information [56]

Equipment	Capacity measure	Base size	Base cost/\$	Cost exponent	$f_M$	$f_P$	$f_T$
Evaporator	Heat transfer area, m <sup>2</sup>	80	32,696	0.68	1.3	1.0	1.6
AH-1	Heat transfer area/m <sup>2</sup>	200	159,117	0.69	1.3	1.0	1.0
Compressor	Power/kW	250	94,947	0.46	1.0	1.0–1.5	1.6–2.1
Condenser	Heat transfer area/m <sup>2</sup>	80	38,254	0.68	1.7	1.0–1.5	1.6–2.1
AH-2	Heat transfer area/m <sup>2</sup>	200	149,990	0.69	1.3	1.0–1.5	1.0
Blower	Power/kW	50	10,924	0.76	1.0	1.0	1.0
Fan	Power/kW	50	10,924	0.76	1.0	1.0	1.0



$$M_{\text{emissions, Fuel}} = (\mu_{\text{CO}_2} + \mu_{\text{SO}_2} + \mu_{\text{NO}_x}) \cdot t_{\text{op}}(\text{Fuel consumption, } N) \quad (30)$$

Emission reduced by WHR as a result of fuel saved can be obtained by modifying previous equation:

$$M_{\text{emissions, Saved}} = (\mu_{\text{CO}_2} + \mu_{\text{SO}_2} + \mu_{\text{NO}_x}) \cdot t_{\text{op}}(\text{Fuel saved, } B) \quad (31)$$

where  $\mu_{\text{CO}_2}$ ,  $\mu_{\text{SO}_2}$ ,  $\mu_{\text{NO}_x}$  are emission factors; their values are given in Table 5.  $t_{\text{op}}$  is the operating time, which is taken as 2880 h. The emissions due to refrigerant leakage or loss during the operating time are obtained from the following equation [59]:

$$\text{Emissions (Refrigerant leakage)} = RC \cdot (LT \cdot ALR + EOL) \cdot GWP \quad (32)$$

where  $RC$  is refrigerant charge (kg),  $LT$  is lifetime of the system (years),  $ALR$  is annual leakage rate (% of  $FC$ ), and  $EOL$  is end of life leakage rate (% of  $FC$ ). Nowadays,  $\text{CO}_2$  penalty cost  $C_{\text{CO}_2}$  is implemented to minimize the emissions. In China,  $\text{CO}_2$  penalty cost is 9 (\$  $\text{ton}^{-1}$ ) [60]. Total penalty cost saved by using WHR is obtained by [34]:

$$Z_{\text{cost}} = m_{\text{CO}_2} \text{CO}_2 \quad (33)$$

where  $m_{\text{CO}_2}$  is the mass of  $\text{CO}_2$  saved in kg.

### Sustainability index (SI)

Efficient utilization of non-renewable energy source (e.g., natural gas) can improve environmental sustainability. The relation between exergy and environment can be well described through sustainability index (SI) [62]:

$$SI = \frac{1}{D_p} \quad (33)$$

where  $D_p$  stands for depletion number, the ratio between exergy destruction and exergy input. This relationship illustrates how to reduce the environmental impact of the system by reducing the exergy destruction.

**Table 5** Fuel and electricity emission factors information [61]

Factor	Natural gas/kg $\text{m}^{-3}$	Electricity/kg $\text{kWh}^{-1}$
$\mu_{\text{CO}_2}$	1.94	0.997
$\mu_{\text{SO}_2}$	0.00124	0.03
$\mu_{\text{NO}_x}$	0.00496	0.015

## Results and discussion

The results obtained for the proposed system are presented in this section.

### Plant specifications

A 31.5-MW natural gas boiler was selected for the proposed system performance test [63]. The boiler is used to provide hot water to a heating area of 400,000  $\text{m}^2$ . The boiler parameters are detailed in Table 6. The schematic of the WHR system equipped with the boiler is shown in Fig. 2.

### Model validation

The model was simulated by using Aspen Plus software. For this purpose, the Peng-Robinson property method is used. The experimental data obtained from the literature are also validated by the same method. The validation of vapor compression heat pump is carried out by adopting the experimental data from the work of Ju et al. [64] for R22 and R744/R290 blend. Figure 3 represents the results for the validation for the effect of heat sink temperature lift on the variation of  $COP$ , compressor work and heating capacity. The percentage average absolute deviation (AAD%) [65] results obtained for the comparison between experimental and simulation data are presented in Table 7. Satisfactory results ( $\pm 10\%$ ) were obtained, which allows the adaptability of the developed model for further study.

### Performance analysis

Main operating parameters of the system obtained for different refrigerants are listed in Table 8. The purpose of using different refrigerants was to examine the increase in return water temperature with minimal compressor work and maximal  $COP$ . It can be seen that the increase in return water temperature for R114 was 54.33  $^{\circ}\text{C}$ , which is highest as compared to the other refrigerants with 1219.62 kW compressor

**Table 6** Information of boiler selected as a test case

Parameter	Value
Flue gas temperature/ $^{\circ}\text{C}$	120
Flue gas flow rate/kg $\text{s}^{-1}$	10.51
Return water temperature/ $^{\circ}\text{C}$	50
Return water flow rate/kg $\text{s}^{-1}$	188.92
Supply water temperature/ $^{\circ}\text{C}$	95
Natural gas flow rate/kg $\text{s}^{-1}$	0.54
Boiler supply air flow rate/kg $\text{s}^{-1}$	9.97
Excess air ratio	1.05

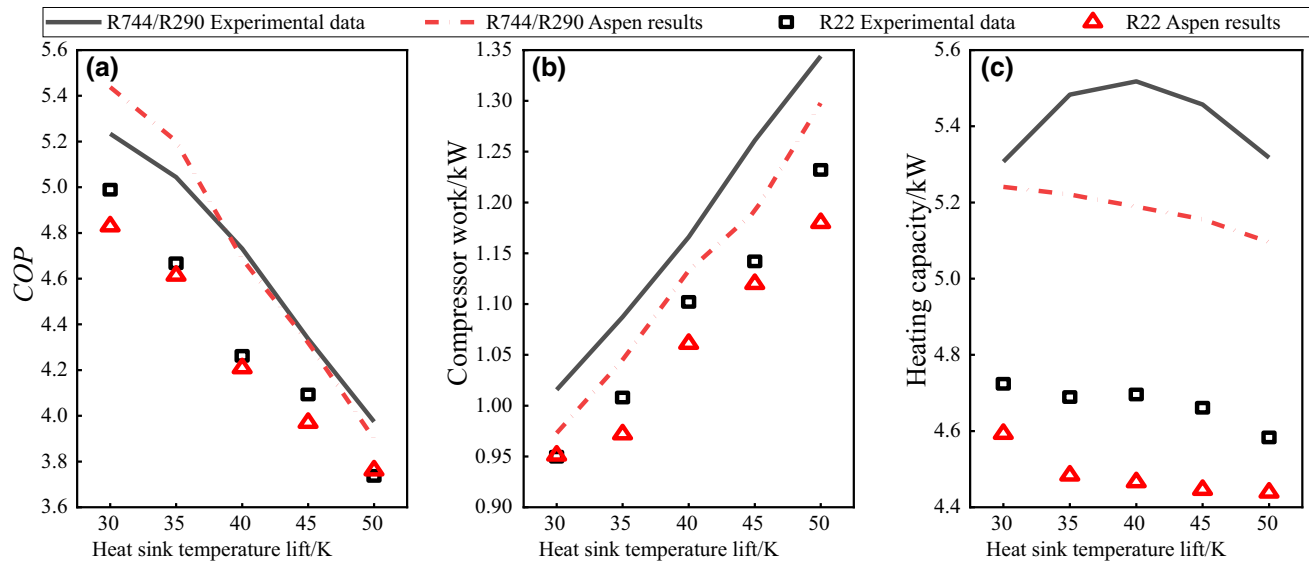


**Fig. 3** The effect of heat sink temperature lift on **a** COP, **b** compressor work, and **c** heating capacity

**Table 7** AAD% results between the experimental and simulated data

Description	AAD% Results	
	For R744/R290	For R22
COP	0.73%	-1.58%
Compressor work	-4.12%	-2.75%
Heating capacity	-4.56%	-3.51%

work. The increase in return water temperature was observed as: R114 > R717 > R744 > R600 > R134a > R1234ze(E) > R1234yf > R245fa > R718 > R1233zd(E), while for compressor work the obtained sequence was R717 > R744 > R114 > R6

00 > R1234yf > R718 > R134a > R1234ze(E) > R245fa > R1233zd(E). Lowest power was consumed by R1233zd(E) at a highest pressure ratio among all other refrigerants. Side by side, the increase in return water temperature (51.34 °C) by R1233zd(E) was also the lowest. The difference between return water temperature and compressor work largely depends on the refrigerant mass flow rate, because the chemical properties of refrigerants (Table 1) have a great influence on the outcomes. In the case of AH-1, the values of air mass flow rate, exit air temperature, flue gas temperature and condensate recovered were almost same. The reason is that AH-1 is the second stage of IDCCU, and the temperature of flue gas exiting the first stage (evaporator) is dropped to

**Table 8** Operating parameters of WHR system for different refrigerants

Parameter	R114	R134a	R245fa	R600	R717	R718	R744	R1233zd(E)	R1234yf	R1234ze(E)
Refrigerant mass flow rate/kg s <sup>-1</sup>	13.98	9.83	9.32	4.76	4.08	0.36	9.98	3.28	9.60	9.40
Return water temperature lift/°C	54.33	53.39	52.68	53.61	54.18	51.87	53.92	51.34	53.11	53.17
Compressor work/kW	1219.62	613.65	453.79	799.81	2855.23	660.94	2667.03	308.41	687.05	584.27
Evaporator pressure/bar	2	3	2	1.2	1.4	0.01	1.5	1.3	2	2
Condenser pressure/bar	16	14	10	10	10	1	10	20	14	11
Flue gas temperature/°C	30.78	30.78	30.78	30.78	30.78	30.78	30.78	30.78	30.78	30.78
AH-1 air temperature/°C	47.84	47.84	47.84	47.84	47.84	47.84	47.84	47.84	47.84	47.84
AH-1 air flow rate/kg s <sup>-1</sup>	37.82	37.82	37.82	37.82	37.82	37.82	37.82	37.82	37.82	37.82
Condensate recovered/%	74.59	74.59	74.59	74.59	74.59	74.59	74.59	74.59	74.59	74.59
AH-2 air temperature/°C*	49	49	49	49	49	11.11	45.40	20.97	49	49
AH-2 air flow rate/kg s <sup>-1</sup>	13.86	14.60	12.59	11.66	10.08	10.00	10.08	10.00	13.61	13.36
Fan work/kW	84.02	84.02	84.02	84.02	84.02	84.02	84.02	84.02	84.02	84.02
Blower work/kW	390.95	396.55	381.42	374.30	362.34	361.74	362.34	361.74	389.05	387.14

\*Boiler supply air temperature

around 52 °C to 55 °C (dew point). Although more heat can be recovered in the first stage of IDCCU, this can increase the compressor work. Moreover, low-temperature flue gas results in reduced AH-1 performance. Therefore IDCC was modeled to extract more heat of flue gas in a performance optimized way. Use of AH-1 was helpful in achieving the hot air for heating area at a temperature of 47.84 °C with 37.82 (kg s<sup>-1</sup>) flow rate. The flue gas temperature was dropped to 30.78 °C and about 2390.24 (kg hr<sup>-1</sup>) or 74.59% water was recovered. AH-2 was introduced to capture the remaining heat from the heat pump. The captured heat was then used for; firstly as a boiler supply air, and secondly for residential heating purpose. As given in Table 6, the return water temperature from heating area at condenser inlet is about 50 °C, so the refrigerant leaving the condenser is at a temperature which is high enough to raise the temperature of an air stream with a specific mass flow rate. Rise in temperature of air stream for most of the refrigerants was 49 °C (minimum 1 °C temperature approach). The lowest rise in air temperature was reported for R718 and R1233zd(E). Airflow rate is set according to the requirement of boiler supply air (9.97 kg s<sup>-1</sup>), because main purpose of AH-2 is to increase the boiler supply air temperature and the remaining air is utilized for heating area. The range of airflow rate for different refrigerants is from 10 to 15 (kg s<sup>-1</sup>). Power consumed by blower to supply the air to WHR system is also important because of its effect on operating cost.

Exergy analysis results for different refrigerants are presented in Fig. 4. Highest exergy efficiency of the system was noted as 61.72% for R245fa, while the lowest exergy efficiency was reported as 22.26% for R744. The order of exergy efficacy is: R245fa > R134a > R1234ze(E) > R1234yf > R114 > R600 > R1233zd(E) > R718 > R717 > R744. It can be observed that the exergy destruction in the condenser is highest. High mass flow rate of return water and the refrigerant phase change caused excessive exergy losses.

Table 9 represents the results for *COP*, heating *COP* and boiler efficiency of the tested refrigerants. The introduction of AH-2 in the heat pump has significantly improved the *COP* of the WHR system. R245fa has a highest *COP* of 6.35, which increased from 5.06 after adding AH-2 (DMS). R717 and R744 had the lowest *COP*, 1.41 and 1.40, respectively. The huge difference in the values is due to the compressor work. On the other side, the highest heating *COP* was noted for R134a (3.27), while lowest *COP* was noted for R744 (1.21). The impact of the system integration on the energy and exergy efficiency of boiler is shown also studied. The results of these efficiencies are strongly dependent on the boiler supply air temperature and return water temperature. The calculated energy and exergy efficiencies of the test case were 81.80% and 64.14%, respectively. An increase of about 10.05% in the energy and 5.83% for the exergy efficiency of boiler was noted for refrigerant R114, which

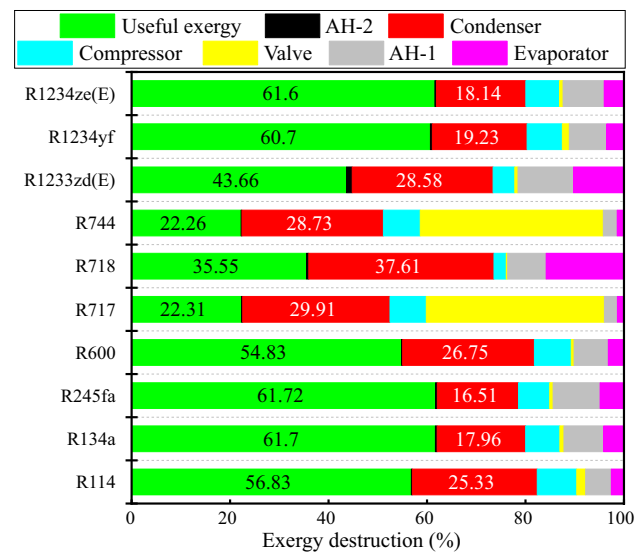


Fig. 4 Exergy destruction in WHR components for simulated refrigerants

is highest among all the refrigerants. The lowest increase in efficiencies was noted for R1233zd(E); the energy and exergy efficiencies were increased up to 0.48%, and 0.19%, respectively.

### Parametric analysis

Parametric analysis was performed to observe the system response. For this purpose, the selected parameters were mass flow rate, temperature, and pressure.

The effect of change in refrigerant mass flow rate on flue gas temperature is shown in Fig. 5. It can be noticed that the change of mass flow rate has a great influence on the flue gas temperature. The breakpoint in the curve is the dew point of flue gas, which changes with the change of refrigerant and its mass flow rate. The dew point for most of the refrigerants is in the range of 52–55 °C. For R718, gas condensation starts at a flow rate of 01 (kg s<sup>-1</sup>). In case of R114, the dew point is 53.62 °C at a flow rate of 11 (kg s<sup>-1</sup>). Excessive mass flow rate of refrigerant can further decrease the flue gas temperature thereby increasing the compressor work. The change effect of refrigerant temperature on flue gas temperature can be observed from Fig. 6. Change in refrigerant temperature for most of the selected refrigerants effect linearly on the flue gas temperature. For a fixed mass flow rate, the flue gas temperature drops between 51 and 52 °C. Refrigerants R134a, R245fa, R600, and R1234ze(E) have shown linear trend for a temperature range of 0–10 °C. For this reason, it is necessary to optimize the mass flow rate of the above-mentioned refrigerants according to the ambient conditions. Optimal

**Table 9** Results of studied refrigerants obtained for COP, heating COP and boiler efficiency

Parameter	R114	R134a	R245fa	R600	R717	R718	R744	R1233zd(E)	R1234yf	R1234ze(E)
<i>COP</i>										
Without AH-2	3.03	4.72	5.06	3.86	1.25	2.42	1.25	3.71	3.87	4.64
With AH-2	3.56	5.83	6.35	4.54	1.41	2.54	1.41	4.28	4.79	5.71
<i>Heating COP</i>										
Without AH-2	2.18	2.62	2.49	2.54	1.08	1.44	1.07	1.52	2.29	2.57
With AH-2	2.56	3.27	3.13	2.88	1.22	1.51	1.21	1.75	2.84	3.16
<i>Boiler efficiency</i>										
Energy efficiency	90.02%	89.91%	89.26%	89.97%	89.95%	82.23%	89.05%	82.19%	89.81%	89.87%
Exergy efficiency	67.88%	67.63%	66.98%	67.75%	67.71%	64.31%	67.13%	64.26%	67.21%	67.45%

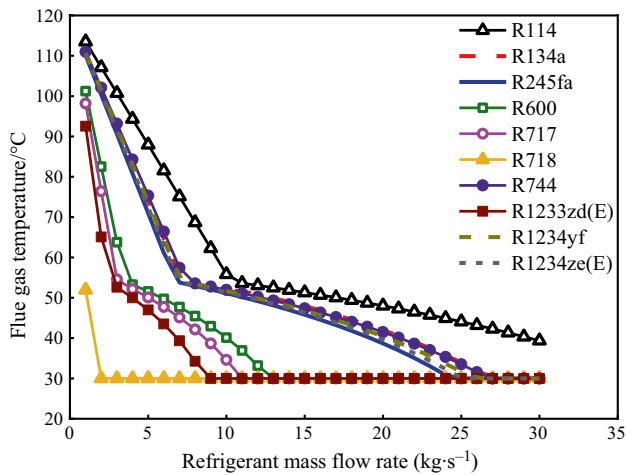


**Fig. 5** Variation effect of refrigerant mass flow rate on flue gas temperature

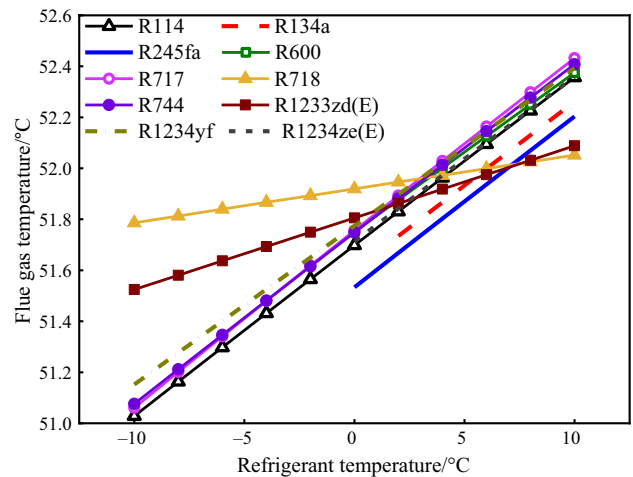


**Fig. 6** Change effect of refrigerant temperature on flue gas temperature

mass flow rate with fluctuating ambient conditions can be helpful in obtaining a desired flue gas temperature at the exit of evaporator. Moreover, maximum COP can be achieved in this way.

The results of variation in the mass flow rate of ambient air for AH-1 are presented in Fig. 7. The effect of this variation on the flue gas temperature, vapor fraction, exit air temperature, and heat exchanger area is discussed. From Fig. 10, it can be observed that the gradual increase in air mass flow rate can help in decreasing the flue gas temperature to a desired limit by maximizing the condensation process. In figure, the trend of heat exchanger area is seemed to be like a cone type shape. The possible reason can be the decrease in flue gas temperature which boosted the condensation of water vapors. The presence of multiphase flow is resulted in the increase of heat exchanger area. In addition, the outlet air temperature line remains unchanged up to a mass flow rate of 35 kg s<sup>-1</sup>. These two factors are the major reasons behind the increase in heat exchanger area. As the mass flow rate exceeds from 35 kg s<sup>-1</sup>, the exit air

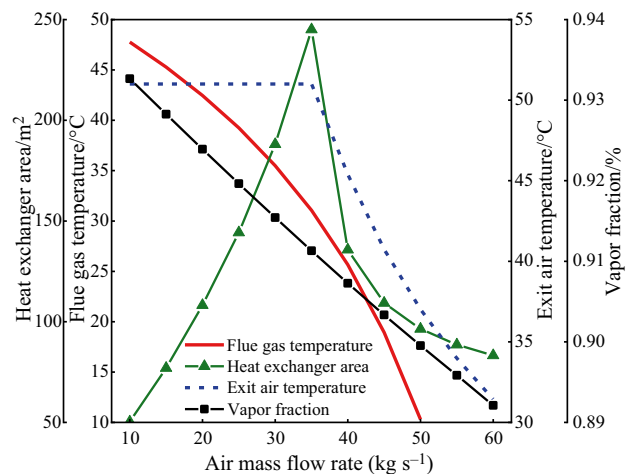


**Fig. 7** Effect of airflow rate on flue gas temperature, vapor fraction, exit air temperature, and heat exchanger area

temperature tends to decrease with the decrease in flue gas temperature by reducing the heat exchanger area. As far as the temperature of air stream is concerned, it is necessary to maintain a suitable temperature enough for residential heating. Fluctuation in ambient conditions can affect the flue gas temperature and vapor fraction (Fig. 8). Cold conditions can assist in decreasing the flue gas temperature but the amount of condensate can be recovered up to a certain limit due to the constant mass flow rate of flue gas. Secondly, high ambient temperature (above 5 °C) can help in maintaining the high temperature of exit area for the cost of heat exchanger area. In cold conditions, less heat exchanger area is required, but the outlet air temperature will be reduced accordingly. Fluctuating weather conditions can be handled by managing the airflow rate. Therefore, the role of airflow rate cannot be underestimated.

The refrigerant pressure in the condenser has a significant effect on the return water temperature lift. Figure 9 shows the trend of the return water temperature increase with the refrigerant pressure. The sudden curves can be seen for most refrigerants. This is because the phase change of the refrigerant that helps in raising the temperature of the returned water. For R717 and R744, since there is no phase change in the condenser, the return water temperature rises steadily. In order to increase the temperature of the return water, a high discharge pressure is required, but the compressor work can increase alternatively. Refrigerant properties have a significant effect on the compressor power consumption. As shown in Fig. 9, compressor work is lowest for R1233zd(E) and highest for R717 among the tested refrigerants. The order of compressor work for the studied refrigerants is: R717 > R744 > R718 > R114 > R600 > R1234yf > R1234ze(E) > R134a > R245fa > R1233zd(E). Although for R1233zd(E) the compressor work is lowest, the increase in return water temperature is also very minimum. Highest return water temperature

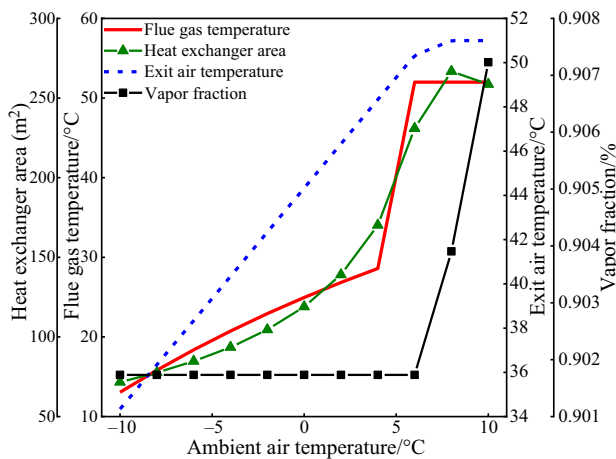


Fig. 8 Effect of ambient air temperature on flue gas temperature, vapor fraction, exit air temperature, and heat exchanger area

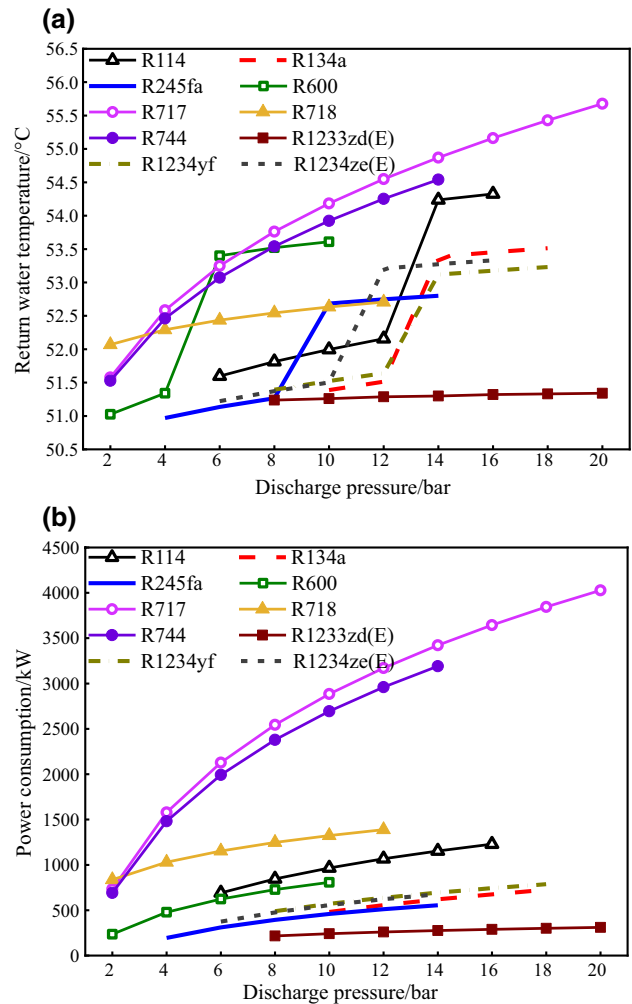
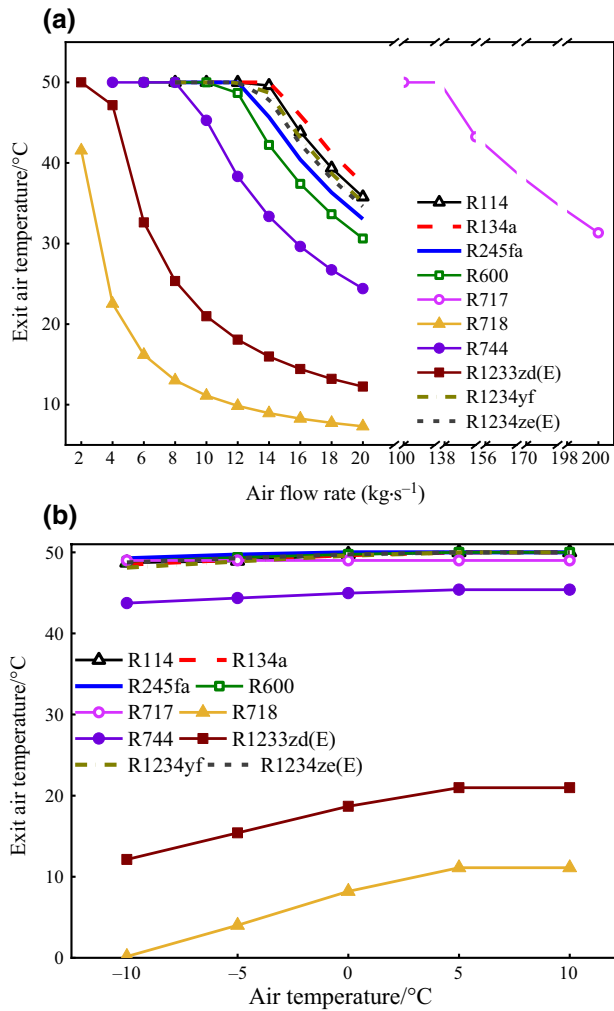


Fig. 9 Effect of discharge pressure on the a rise in return water temperature and b compressor power consumption

(54.33 °C) was observed for R114 at 20 bar pressure. From the above discussion, we can conclude that the pressure of refrigerant significantly affect the return water temperature, but the compressor work should be kept in mind to avoid unnecessary power cost.

AH-2 was introduced in the heat pump to reduce the internal heat loss and acts as a mechanical sub-cooler, as discussed in earlier sections. The air mass flow rate was set according to the boiler supply air requirements (9.97 kg s<sup>-1</sup>). The effect of variation in air mass flow rate and the fluctuation in ambient air temperature on exit air temperature is shown in Fig. 10. Nine refrigerants responded against the mass flow rate when the mass flow rate of air varied from 2 to 20 (kg s<sup>-1</sup>), while the variation in the exit air temperature for R717 started at air mass flow rate around 120 (kg s<sup>-1</sup>) (Fig. 10). This is because of the phase change that occurred in AH-2 for R717 as a result of high mass flow rate of air. The exit air temperature for most of the refrigerants is above





**Fig. 10** Variation in exit air temperature influenced by refrigerants due to **a** change in air flow rate and **b** change in ambient air temperature

48 °C with a slight variation against ambient conditions, while for R718, the exit air temperature was set at 11.11 °C which is the lowest (Fig. 10). Due to the minimal impact of environmental conditions, the air mass flow can be changed according to the needs of indoor heating. Alternatively, the boiler supply air temperature will decrease by increasing the natural gas consumption. The effect of boiler supply air temperature on fuel consumption is discussed in forthcoming section.

The effect of compressor discharge pressure on the *COP* of the WHR system is illustrated in Fig. 11. As the discharge pressure increases, the *COP* of the system tends to decrease. This trend can be observed for all the tested refrigerants. This is because of the two stage rejection from the refrigerant; firstly in condenser and secondly in AH-2. At low pressure the refrigerant temperature is insufficient to rise the return water temperature due to the high mass flow rate

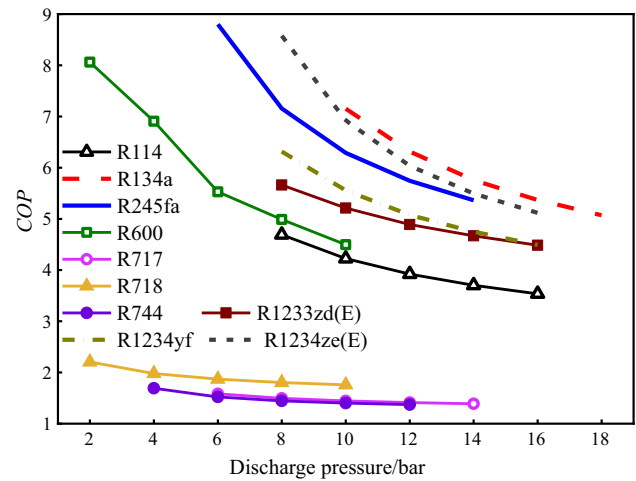


**Fig. 11** Effect of discharge pressure on the *COP* of WHR system

(188.82 kg s<sup>-1</sup>). Therefore, most of the refrigerant heat is rejected in AH-2, which results in high *COP* at low pressure. As the refrigerant pressure increases, due to the phase change of the refrigerant, the maximum heat is absorbed by the return water in the condenser. The remaining heat of the refrigerant is captured by the boiler supply air, as discussed earlier in this section. In contrast, refrigerants R744, R718, and R717 have the lowest *COP*. In a nut shell, the selection of refrigerant is the key factor of cost effective performance for the WHR system.

### Cost analysis

The performance of the proposed system largely depends on the operating parameters and ambient conditions. It is possible to achieve the desired results, but this can result in increased plant cost by reducing the payback period and profit. The overall plant cost is a major influencing factor toward the success or failure of the system due to its impact on payback period. In the case of heat pumps, plant cost is mainly dependent on the equipment cost, which varies due to the variation in some vital parameters, such as pressure, temperature, and equipment material. The results of plant cost for different refrigerants and corresponding influence of each refrigerant with respect to operating cost and the associated payback period can be observed from Fig. 12. It can be noticed that the plant cost is higher for R134a and the payback period (calculated on the basis of heating seasons, 01 heating season is comprised of 24 h operating time in a day for 120 days) is also higher (slightly lower than R717), which is around 13 heating seasons. In the case of R1233zd(E), the plant cost is lower and the payback period is also minimum. This is due to the cost of electricity consumption by compressor and auxiliaries, which is higher in the case of R717 and



R134a. In the case of savings per heating season at the end of payback period, the maximum profit can be achieved if R114 is used as a working fluid in the proposed system due to its capacity to lift the return water temperature up to maximum among the other tested refrigerants. The comparative results of plant cost and savings after the payback period can be observed from Fig. 12. Refrigerants R717, R718, R744, and R1233zd(E) have the lowest potential toward economic profit. In the case of R717 and R744, the compressor power consumption is very high which tends toward the increase in operating cost, hence by decreasing the profit. In the case of R1233zd(E) and R718, the compressor work is comparatively lower than R717 and R744, but their impact toward rising the temperature of return water is very lower; that is why they offer lesser savings.

Fuel saving can greatly contribute toward the cost and emission reduction. In the case of proposed system integrated with the developed case study, the fuel cost saving potential based on heating season can be observed from Table 10. It can be seen that maximum fuel cost can be saved if the proposed system is operated with R114. This is due to the maximum increase in return water temperature from 50 °C to 54.33 °C, which was obtained by using R114. Moreover, it can be noticed that the minimal fuel cost saving was noted for R1233zd(E) and R718 due to the same reason (lesser potential to rise the return water temperature).

In order to simplify the economics of proposed system, the method of benefit-to-cost ratio analysis (*BCRA*) is adopted. In this method, the obtainable cost benefits are divided by the expenses (cost). In this work, the benefits are the savings that can be achieved in the form of costs saved by reducing the fuel consumption and associated carbon tax. On the other side, the operating and maintenance costs are covered in expenses. *BCRA* is a unit less factor because both the benefits and expenses are taken into a specific currency. In this work, dollar (\$) is used as a currency. The value of *BCRA* decides the status of a project if it will result in a positive return, negative return or will be cost neutral. A *BCRA* value higher than 01 means that positive return or profit can be expected from the project and vice versa. The results of *BCRA* ratio for the tested refrigerants can be observed through Table 11. It can be noticed that positive return is expected for about 08 refrigerants, in which the maximum profit can be obtained by using R245fa. Loss from the project can be expected if refrigerants R717 and R744 are adopted, and this is due to their higher operating costs (higher compressor work).

### Environmental analysis

Waste heat recovery systems have a great impact on the environment due to their capability of emission reduction. They assist in reducing the harmful emissions (CO<sub>2</sub>, SO<sub>2</sub>,

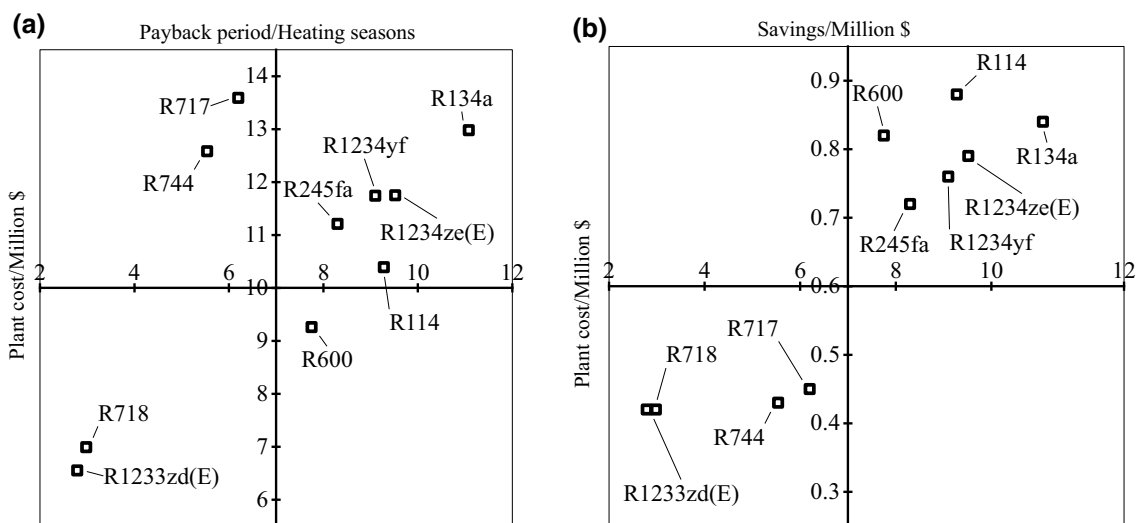


Fig. 12 Influence of plant cost on a payback period and b associated savings, measured for the selected refrigerants

Table 10 Fuel cost saving potential of studied refrigerants

	R114	R134a	R245fa	R600	R717	R718	R744	R1233zd(E)	R1234yf	R1234ze(E)
Fuel cost saved (million \$)	1.21	1.04	0.89	1.06	1.16	0.62	1.10	0.54	0.98	0.99

**Table 11** The results of BCRA analysis for the studied refrigerants

	R114	R134a	R245fa	R600	R717	R718	R744	R1233zd(E)	R1234yf	R1234ze(E)
BCRA	2.48	3.60	3.69	3.09	0.71	1.79	0.72	2.57	3.09	3.54

**Fig. 13** Percentage emission reduced by the tested refrigerants (per heating season)

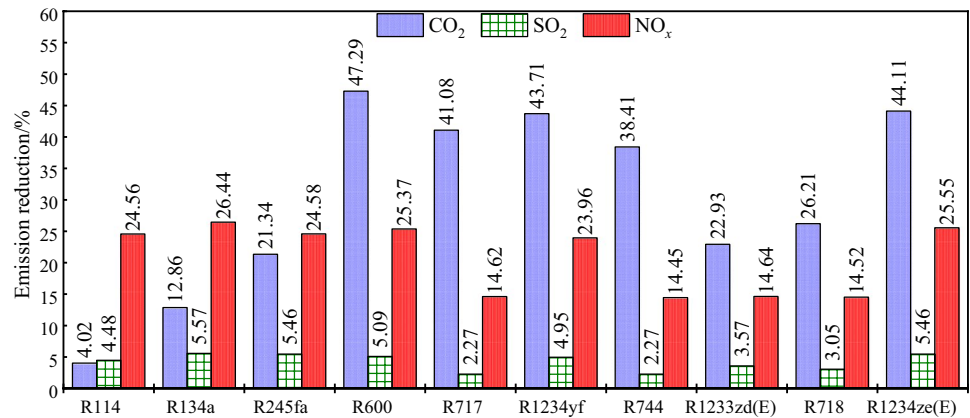


**Table 12** Carbon tax saved per heating season

	R114	R134a	R245fa	R600	R717	R718	R744	R1233zd(E)	R1234yf	R1234ze(E)
Carbon tax saved ( $\times 10^3$ \$)	3.96	10.58	14.72	40.87	38.86	11.92	34.30	8.71	33.66	34.41

**Table 13** Sustainability index (SI) of the WHR system for the tested refrigerants

	R114	R134a	R245fa	R600	R717	R718	R744	R1233zd(E)	R1234yf	R1234ze(E)
SI	2.32	2.61	2.61	2.21	1.29	1.55	1.29	1.77	2.54	2.60

and NO<sub>x</sub>) by minimizing the fuel consumption with effective utilization of recovered waste heat. The emissions related to the electricity consumption are still an issue. By considering these factors, an environmental study on the presented system is conducted for the selected refrigerants. The emission reduction potential (%) of different refrigerants when tested in the proposed system is presented in Fig. 13. Carbon dioxide is considered a major pollutant that contributes to global warming. Around 47.29% of CO<sub>2</sub> emissions can be reduced during a heating season if the WHR is operated with R600. Although R114 has the highest potential to increase the boiler supply air temperature, due to its higher GWP value, it has lesser emission reduction potential among the other tested refrigerants. Nowadays, carbon tax is implemented by the governments if the amount of CO<sub>2</sub> emissions exceed the set limit. Reasonable results are obtained after this measure. For the current case, cost analysis results related to CO<sub>2</sub> emissions are presented in Table 12. Handsome amount of cost can be saved during a heating season which can increase the overall benefits. Finally, it can be yielded that the addition of the proposed system is a

useful approach toward environmental sustainability and cost saving.

### Sustainability analysis (SI)

The results of sustainability analysis are presented in Table 13. Refrigerants R134a and R245fa have the highest SI value of 2.61, R717 and R744 have the lowest value of 1.29. Highest SI means that lesser exergy destruction and vice versa. The order of SI is: R1234a = R245fa > R1234ze (E) > R1234yf > R114 > R600 > R1233zd(E) > R718 > R717 > R744.

### Refrigerant selection approach

In order to select a refrigerant, a new approach is introduced which is based on COP, SI, and BCRA. BCRAR stands for benefit-to-cost (expense) ratio, as discussed earlier. Profit and the carbon tax saved per heating season are considered

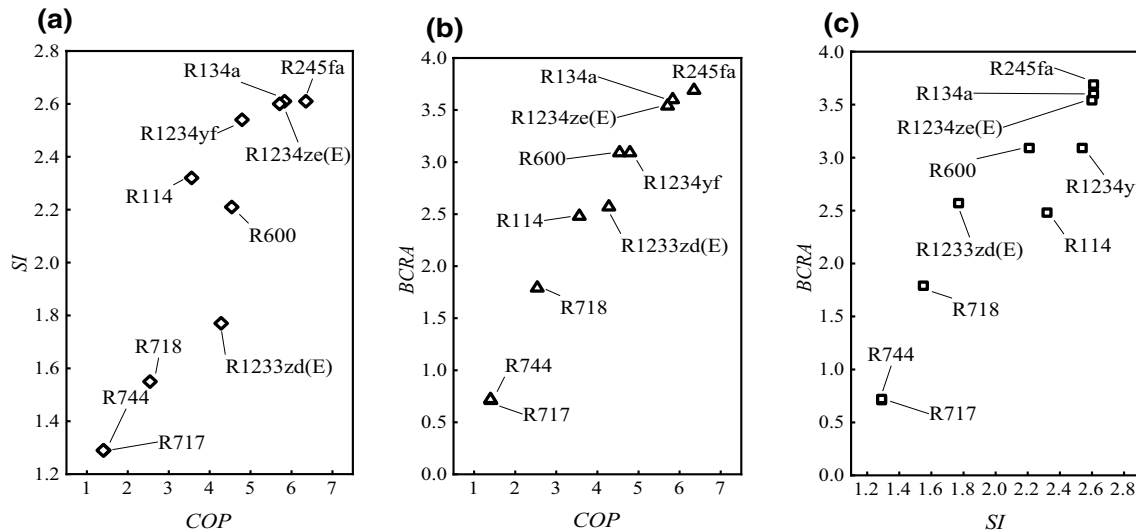


**Fig. 14** Selection of the best suitable refrigerant for the WHR system by comparison between **a**  $COP$  and  $SI$ , **b**  $COP$  and  $BCRA$ , and **c**  $SI$  and  $BCRA$

as the benefits obtained from the proposed system for a specific refrigerant, while the operating and maintenance cost during the entire heating season is taken as expenses. The comparison between these three parameters is based on the performance, environmental impact, and the cost factor of the proposed system. The reason behind choosing these three parameters is their influence.  $COP$  helps in determining the performance of heat pump cycle which varies the under fluctuating weather conditions.  $SI$  helps in measuring the useful energy conversion by keeping an eye on the reduction of energy wastage, while  $BCRA$  method can provide a clear guidance about a system that either it is suitable or not by keeping in mind the economics. Therefore, in general, these three parameters independently focus on the three E's (EEE), which are energy, environment, and economics. The combination of these parameters in a simplified way can help us in selecting the best suitable working fluid for the proposed system. In order to obtain the further information about this approach, Fig. 14 represents the comparison results between  $COP$ ,  $SI$  and  $BCRA$ . If we put a look on the comparison between  $SI$  and  $COP$  (Fig. 14), it can be seen that the refrigerant R245fa has the highest  $COP$  among other refrigerants, while R134a is the second. On the other hand, R245fa and R134a both have the same  $SI$  value. On the other hand, in the case of comparison between  $BCRA$  and  $COP$  (Fig. 14), the  $BCRA$  value is higher for R245fa, while R134a and R1234ze(E) are at the second and third places, respectively. In the case of  $BCRA$  and  $SI$  (Fig. 14), almost the same results were obtained. As a conclusion, the comparison results shows that R245fa is the best suitable refrigerant for the proposed system because it has the highest values of  $COP$ ,  $SI$ , and  $BCRA$ . R134a and R1234ze(E) have the minor difference and are at the second and third

positions, respectively. R744 and R717 are at the last position in the list of tested refrigerants. Further, it can be said that the selection of a suitable refrigerant through  $COP$ ,  $SI$ , and  $BCRA$  analysis is very helpful and the analysis can be used in other engineering case studies by replacing some parameters. For example, in the case of organic Rankine cycle (ORC), the  $COP$  can be replaced with the cycle efficiency or power generation capacity. Although the other two parameters will remain unchanged, their corresponding values will be obtained as per the procedure.

## Conclusions

In this study, the performance assessment of a novel hybrid heat pump system was carried out by using ten refrigerants. The system was proposed for domestic heating applications after its modification with an integrated multistage condensing economizer and dedicated mechanical sub-cooler (DMS). The study results have shown the significant improvement in the reduction of internal heat losses and compressor power consumption, which are discussed below.

- The integration of proposed heat pump system with the domestic heating boiler was a positive aspect toward the increase in energy and exergy efficiency of the boiler. It was noted that the return water temperature could be increased from 50 to 54.33 °C if the proposed system is operated with refrigerant R114. In addition to that, the introduction of AH-2 in the heat pump cycle significantly increased the temperature of boiler supply air by reducing the internal heat losses of heat pump. The boiler supply air temperature was raised from ambient to around 49

°C. These two factors collectively increased the energy and exergy efficiency of the boiler from 81.8% to 92.13% and 64.14% to 68.91%, respectively. Besides these positive factors, R114 has lesser emission reduction potential due to its higher GWP value, which makes it not suitable for use.

- The exergy destruction was maximum in the condenser due to large amount of return water from heating area ( $188.92 \text{ kg}\cdot\text{s}^{-1}$ ). Highest exergy efficiency was noted for refrigerant R245fa, which was 61.72%, while the exergy efficiency for R134a, R1234ze(E) and R1234yf was 61.70%, 61.70%, and 61.60%, respectively.
- Due to the addition of AH-2 (dedicated mechanical sub-cooler) in the heat pump, a significant improvement in the *COP* was noted. The *COP* of heat pump cycle with and without AH-2 was compared for tested refrigerants. Maximum *COP* was noted for R245fa, which was 6.35 with AH-2 and 5.06 without AH-2 (25.58% increase), while the maximum heating *COP* was noted for R134a, which was 3.27 with AH-2 and 2.62 without AH-2 (24.81% increase).
- Parametric study results show that the variation in key parameters such as flow rate and pressure is dependent on the ambient conditions, which then have an influence on *COP*, exergy efficiency, and economics. It was further noted that with the increase in refrigerant discharge pressure the *COP* of the system tends to decrease due to the increase in compressor power consumption. For R600, a decrease in *COP* from 8.06 to 4.49 was noted because of the change in discharge pressure from 2 to 10 bar, while the power consumption increased from 235.06 kW (at 2 bar) to 807.89 kW (at 10 bar).
- While conducting a comparative study to select the suitable working fluid, random results are expected for different refrigerants, which makes the selection even harder. To cater this problem, a novel performance-sustainability-cost based approach was introduced. As a result, R245fa was selected as a suitable refrigerant for the proposed system, while R134a and R1234ze(E) were selected at a second space. Moreover, the proposed method can also be adopted for the selection of working fluid in the case of organic Rankine cycle, vapor absorption heat pump, and many other thermodynamic cycles, because performance, sustainability, and economics are the main deciding factors in plant selection.

Lastly, it can be said that the proposed system has a potential to minimize the internal waste heat losses of heat pumps and other hybrid thermodynamic cycles where internal heat recovery can be very much beneficial (technically and economically). We hope that this research work will open the new ways of thinking toward the minimization of internal waste heat losses. Further research work on this topic is also

expected, which will be focused on the introduction of more refrigerants and nano-fluids.

**Authors contribution** SRJ was involved in the conceptualization, methodology, software, validation, data curation, and writing—original draft. LW contributed to the formal analysis, investigation, methodology, and writing—review and editing. HSA was involved in the data curation and writing—review and editing. DC was involved in the supervision, funding acquisition, project administration, and writing—review and editing.

**Funding** The financial support from the National Natural Science Foundation of China (Grant No. 51806171) is gratefully acknowledged. The authors also appreciate the study support provided by Xi'an Jiaotong University.

## Declarations

**Conflicts of interest** The authors declared that they have no conflict of interest.

## References

1. IEA. Carbondioxide emission from fuels combustion, International Energy Agency, OECD, Paris. 2017.
2. Allen MR, Stocker TF. Impact of delay in reducing carbon dioxide emissions. *Nat Clim Chang*. 2014;4:23–6. <https://doi.org/10.1038/nclimate2077>.
3. Kim K-H, Jahan SA, Kabir E. A review of diseases associated with household air pollution due to the use of biomass fuels. *J Hazard Mater*. 2011;192:425–31. <https://doi.org/10.1016/J.JHAZMAT.2011.05.087>.
4. Jouhara H. Waste heat recovery technologies and applications waste heat recovery technologies and applications. *Therm Sci Eng Prog*. 2018. <https://doi.org/10.1016/j.tsep.2018.04.017>.
5. Jeong K, Kessen MJ, Bilirgen H, Levy EK. Analytical modeling of water condensation in condensing heat exchanger. *Int J Heat Mass Transf*. 2010;53:2361–8. <https://doi.org/10.1016/j.ijheatmasstransfer.2010.02.004>.
6. Barma MC, Saidur R, Rahman SMA, Allouhi A, Akash BA, Sait SM. A review on boilers energy use, energy savings, and emissions reductions. *Renew Sustain Energy Rev*. 2017;79:970–83. <https://doi.org/10.1016/j.rser.2017.05.187>.
7. Wan H, Cao T, Hwang Y, Oh S. A review of recent advancements of variable refrigerant flow air-conditioning systems. *Appl Therm Eng*. 2020. <https://doi.org/10.1016/j.applthermaleng.2019.114893>.
8. Lun YHV, Tung SLD. *Heat Pumps for Sustainable Heating and Cooling*. Berlin: Springer; 2020.
9. Jamil SR, Wang L, Che D. Techno-economic analysis of a novel hybrid heat pump system to recover waste heat and condensate from the low-temperature boiler exhaust gas. *Int J Energy Res*. 2020. <https://doi.org/10.1002/er.5172>.
10. Luo B, Zou P. Performance analysis of different single stage advanced vapor compression cycles and refrigerants for high temperature heat pumps. *Int J Refrig*. 2019;104:246–58. <https://doi.org/10.1016/j.ijrefrig.2019.05.024>.
11. Cooper SJG, Hammond GP, Hewitt N, Norman JB, Tassou SA, Youssef W. Energy saving potential of high temperature

- heat pumps in the UK Food and Drink sector. *Energy Procedia*. 2019;161:142–9. <https://doi.org/10.1016/j.egypro.2019.02.073>.
12. Todorović D, Tomić M, Bojanić R, Bajatović D, Anđelković AS. A comparative analysis of a heat pump application with grey wastewater source for domestic hot water preparation in hotels. *J Therm Anal Calorim*. 2020;141:559–72. <https://doi.org/10.1007/s10973-020-09495-0>.
  13. Bergamini R, Jensen JK, Elmegaard B. Thermodynamic competitiveness of high temperature vapor compression heat pumps for boiler substitution. *Energy*. 2019;182:110–21. <https://doi.org/10.1016/j.energy.2019.05.187>.
  14. Mateu-Royo C, Sawalha S, Mota-Babiloni A, Navarro-Esbrí J. High temperature heat pump integration into district heating network. *Energy Convers Manag*. 2020;210: 112719. <https://doi.org/10.1016/j.enconman.2020.112719>.
  15. Deymi-Dashtebayaz M, Maddah S, Goodarzi M, Maddah O. Investigation of the effect of using various HFC refrigerants in geothermal heat pump with residential heating applications. *J Therm Anal Calorim*. 2020;141:361–72. <https://doi.org/10.1007/s10973-020-09539-5>.
  16. Bamigbetan O, Eikevik TM, Nekså P, Bantle M, Schlemminger C. The development of a hydrocarbon high temperature heat pump for waste heat recovery. *Energy*. 2019;173:1141–53. <https://doi.org/10.1016/j.energy.2019.02.159>.
  17. Song Y, Li D, Cao F, Wang X. Theoretical investigation on the combined and cascade CO<sub>2</sub>/R134a heat pump systems for space heating. *Appl Therm Eng*. 2017;124:1457–70. <https://doi.org/10.1016/j.applthermaleng.2017.06.014>.
  18. Ma X, Zhang Y, Li X, Zou H, Deng N, Nie J, et al. Experimental study for a high efficiency cascade heat pump water heater system using a new near-zeotropic refrigerant mixture. *Appl Therm Eng*. 2018;138:783–94. <https://doi.org/10.1016/j.applthermaleng.2017.12.124>.
  19. D'Agaro P, Cortella G, Polzot A. R744 booster integrated system for full heating supply to supermarkets. *Int J Refrig*. 2018;96:191–200. <https://doi.org/10.1016/j.jrefrig.2018.09.028>.
  20. Mota-Babiloni A, Mateu-Royo C, Navarro-Esbrí J, Molés F, Amat-Albuixech M, Barragán-Cervera Á. Optimisation of high-temperature heat pump cascades with internal heat exchangers using refrigerants with low global warming potential. *Energy*. 2018;165:1248–58. <https://doi.org/10.1016/j.energy.2018.09.188>.
  21. Fukuda S, Kondou C, Takata N, Koyama S. Low GWP refrigerants R1234ze(E) and R1234ze(Z) for high temperature heat pumps. *Int J Refrig*. 2014;40:161–73. <https://doi.org/10.1016/j.jrefrig.2013.10.014>.
  22. Maddah S, Safaei MR. Determination of the optimal discharge pressure of the transcritical CO<sub>2</sub> heat pump cycles for heating and cooling performances based on new correlation. *J Therm Anal Calorim*. 2021. <https://doi.org/10.1007/s10973-021-10723-4>.
  23. Urbanucci L, Bruno JC, Testi D. Thermodynamic and economic analysis of the integration of high-temperature heat pumps in tri-generation systems. *Appl Energy*. 2019;238:516–33. <https://doi.org/10.1016/j.apenergy.2019.01.115>.
  24. Pitarch M, Hervas-Blasco E, Navarro-Peris E, Corberán JM. Exergy analysis on a heat pump working between a heat sink and a heat source of finite heat capacity rate. *Int J Refrig*. 2019;99:337–50. <https://doi.org/10.1016/j.jrefrig.2018.11.044>.
  25. Sarafraz MM, Goodarzi M, Tlili I, Alkanhal TA, Arjomandi M. Thermodynamic potential of a high-concentration hybrid photovoltaic/thermal plant for co-production of steam and electricity. *J Therm Anal Calorim*. 2021;143:1389–98. <https://doi.org/10.1007/s10973-020-09914-2>.
  26. Mehrdad S, Dadsetani R, Amiriyoon A, Leon AS, Safaei MR, Goodarzi M. Exergo-economic optimization of organic rankine cycle for saving of thermal energy in a sample power plant by using of strength pareto evolutionary algorithm II. *Processes*. 2020. <https://doi.org/10.3390/pr8030264>.
  27. Sheikholeslami M, Jafaryar M. Nanoparticles for improving the efficiency of heat recovery unit involving entropy generation analysis. *J Taiwan Inst Chem Eng*. 2020;115:96–107. <https://doi.org/10.1016/j.jtice.2020.09.033>.
  28. Sheikholeslami M, Jafaryar M, Said Z, Alsabery AI, Babazadeh H, Shafee A. Modification for helical turbulator to augment heat transfer behavior of nanomaterial via numerical approach. *Appl Therm Eng*. 2021;182: 115935. <https://doi.org/10.1016/j.applthermaleng.2020.115935>.
  29. Goodarzi M, Toghraie D, Reiszadeh M, Afrand M. Experimental evaluation of dynamic viscosity of ZnO–MWCNTs/engine oil hybrid nanolubricant based on changes in temperature and concentration. *J Therm Anal Calorim*. 2019;136:513–25. <https://doi.org/10.1007/s10973-018-7707-8>.
  30. Bahiraei M, Jamshidmofid M, Goodarzi M. Efficacy of a hybrid nanofluid in a new microchannel heat sink equipped with both secondary channels and ribs. *J Mol Liq*. 2019;273:88–98. <https://doi.org/10.1016/j.molliq.2018.10.003>.
  31. Yarmand H, Gharehkhani S, Shirazi SFS, Goodarzi M, Amiri A, Sarsam WS, et al. Study of synthesis, stability and thermo-physical properties of graphene nanoplatelet/platinum hybrid nanofluid. *Int Commun Heat Mass Transf*. 2016;77:15–21. <https://doi.org/10.1016/j.icheatmasstransfer.2016.07.010>.
  32. Giwa SO, Sharifpur M, Goodarzi M, Alsulami H, Meyer JP. Influence of base fluid, temperature, and concentration on the thermo-physical properties of hybrid nanofluids of alumina–ferrofluid: experimental data, modeling through enhanced ANN, ANFIS, and curve fitting. *J Therm Anal Calorim*. 2021;143:4149–67. <https://doi.org/10.1007/s10973-020-09372-w>.
  33. Afridi MI, Tlili I, Goodarzi M, Osman M, Khan NA. Irreversibility analysis of hybrid nanofluid flow over a thin needle with effects of energy dissipation. *Symmetry (Basel)*. 2019. <https://doi.org/10.3390/sym11050663>.
  34. Xu Y, Jiang N, Pan F, Wang Q, Gao Z, Chen G. Comparative study on two low-grade heat driven absorption-compression refrigeration cycles based on energy, exergy, economic and environmental (4E) analyses. *Energy Convers Manag*. 2017;133:535–47. <https://doi.org/10.1016/j.enconman.2016.10.073>.
  35. Liu X, Yang X, Yu M, Zhang W, Wang Y, Cui P, et al. Energy, exergy, economic and environmental (4E) analysis of an integrated process combining CO<sub>2</sub> capture and storage, an organic Rankine cycle and an absorption refrigeration cycle. *Energy Convers Manag*. 2020. <https://doi.org/10.1016/j.enconman.2020.112738>.
  36. Deymi-Dashtebayaz M, Valipour-Namanlo S. Thermoeconomic and environmental feasibility of waste heat recovery of a data center using air source heat pump. *J Clean Prod*. 2019;219:117–26. <https://doi.org/10.1016/j.jclepro.2019.02.061>.
  37. Maddah S, Deymi-Dashtebayaz M, Maddah O. 4E analysis of thermal recovery potential of industrial wastewater in heat pumps: An invisible energy resource from the Iranian casting industry sector. *J Clean Prod*. 2020;265: 121824. <https://doi.org/10.1016/j.jclepro.2020.121824>.
  38. Jain V, Sachdeva G, Kachhwaha SS. Energy, exergy, economic and environmental (4E) analyses based comparative performance study and optimization of vapor compression-absorption integrated refrigeration system. *Energy*. 2015;91:816–32. <https://doi.org/10.1016/j.energy.2015.08.041>.
  39. Liu S, Li Z, Dai B, Zhong Z, Li H, Song M, et al. Energetic, economic and environmental analysis of air source transcritical CO<sub>2</sub> heat pump system for residential heating in China. *Appl Therm Eng*. 2019;148:1425–39. <https://doi.org/10.1016/j.applthermaleng.2018.08.061>.



40. Maddah S, Goodarzi M, Safaei MR. Comparative study of the performance of air and geothermal sources of heat pumps cycle operating with various refrigerants and vapor injection. *Alexandria Eng J.* 2020;59:4037–47. <https://doi.org/10.1016/j.aej.2020.07.009>.
41. Dadsetani R, Sheikhzadeh GA, Safaei MR, Alnaqi AA, Amirioyon A. Exergoeconomic optimization of liquefying cycle for noble gas argon. *Heat Mass Transf Und Stoffuebertragung.* 2019;55:1995–2007. <https://doi.org/10.1007/s00231-018-2501-5>.
42. Arpagaus C, Bless F, Uhlmann M, Schiffmann J, Bertsch SS. High temperature heat pumps: market overview, state of the art, research status, refrigerants, and application potentials. *Energy.* 2018;152:985–1010. <https://doi.org/10.1016/j.energy.2018.03.166>.
43. Wu D, Yan H, Hu B, Wang RZ. Modeling and simulation on a water vapor high temperature heat pump system. *Energy.* 2019;168:1063–72. <https://doi.org/10.1016/j.energy.2018.11.113>.
44. Liu Y, Han J, You H. Exergoeconomic analysis and multi-objective optimization of a CCHP system based on LNG cold energy utilization and flue gas waste heat recovery with CO<sub>2</sub> capture. *Energy.* 2019. <https://doi.org/10.1016/j.energy.2019.116201>.
45. Che D, Liu Y, Gao C. Evaluation of retrofitting a conventional natural gas fired boiler into a condensing boiler. *Energy Convers Manag.* 2004;45:3251–66. <https://doi.org/10.1016/j.enconman.2004.01.004>.
46. Qu M, Abdelaziz O, Yin H. New configurations of a heat recovery absorption heat pump integrated with a natural gas boiler for boiler efficiency improvement. *Energy Convers Manag.* 2014;87:175–84. <https://doi.org/10.1016/j.enconman.2014.06.083>.
47. Wang J, Hua J, Fu L, Wang Z, Zhang S. A theoretical fundamental investigation on boilers equipped with vapor-pump system for flue-gas heat and moisture R. *Energy.* 2019;171:956–70.
48. Terhan M, Comakli K. Energy and exergy analyses of natural gas-fired boilers in a district heating system. *Appl Therm Eng.* 2017;121:380–7. <https://doi.org/10.1016/j.applthermaleng.2017.04.091>.
49. Maalouf S, Boulawz Ksayer E, Clodic D. Investigation of direct contact condensation for wet flue-gas waste heat recovery using organic Rankine cycle. *Energy Convers Manag.* 2016;107:96–102. <https://doi.org/10.1016/j.enconman.2015.09.047>.
50. Cox KR, Chapman WG. The properties of gases and liquids, 5th Edition By Bruce E. Poling (University of Toledo), John M. Prausnitz (University of California at Berkeley), and John P. O'Connell (University of Virginia). McGraw-Hill: New York. 2001. 768 pp. \$115.00. ISBN 0–07–. vol. 123. 2001. <https://doi.org/10.1021/ja0048634>.
51. Shah RK, Sekulic DP. *Fundamentals of heat exchanger design.* New Jersey: Wiley; 2003.
52. Farshi LG, Khalili S. Thermoeconomic analysis of a new ejector boosted hybrid heat pump (EBHP) and comparison with three conventional types of heat pumps. *Energy.* 2019;170:619–35. <https://doi.org/10.1016/j.energy.2018.12.155>.
53. Sauer, Harry J.; Howell, Ronald Hunter; Coad WJ. *Principles of heating ventilating and air conditioning.* ASHRAE; 2013.
54. Liu F. Review of AC, heat pump and refrigeration systems using natural refrigerants. In: W. H, G. Z, editors. 11th IIR Gustav Lorentzen Conf. Nat. Refrig. GL 2014, Shanghai University of Electric Power, 2103 Pingliang Road, Yangpu District, Shanghai, 200090, China: International Institute of Refrigeration; 2014, p. 569–76.
55. Garousi Farshi L, Mahmoudi SMS, Rosen MA, Yari M, Amidpour M. Exergoeconomic analysis of double effect absorption refrigeration systems. *Energy Convers Manag.* 2013;65:13–25. <https://doi.org/10.1016/j.enconman.2012.07.019>.
56. Smith R. *Chemical process design and integration.* New Jersey: John Wiley & Sons Ltd; 2016.
57. Zhang G, Xiao H, Zhang P, Wang B, Li X, Shi W, et al. Review on recent developments of variable refrigerant flow systems since 2015. *Energy Build.* 2019;198:444–66. <https://doi.org/10.1016/j.enbuild.2019.06.032>.
58. David R, Ngulube P, Dube A. A cost-benefit analysis of document management strategies used at a financial institution in Zimbabwe: a case study. *SA J Inf Manag.* 2013;15:1–10. <https://doi.org/10.4102/sajim.v15i2.540>.
59. Zhang C, Liu C, Xu X, Li Q, Wang S. Energetic, exergetic, economic and environmental (4E) analysis and multi-factor evaluation method of low GWP fluids in trans-critical organic Rankine cycles. *Energy.* 2019;168:332–45. <https://doi.org/10.1016/j.energy.2018.11.104>.
60. Zhu N, Qian L, Jiang D, Mbroh N. A simulation study of China's imposing carbon tax against American carbon tariffs. *J Clean Prod.* 2020;243: 118467. <https://doi.org/10.1016/j.jclepro.2019.118467>.
61. Zhang Q, Zhang L, Nie J, Li Y. Techno-economic analysis of air source heat pump applied for space heating in northern China. *Appl Energy.* 2017;207:533–42.
62. Ahmadi P, Dincer I, Rosen MA. Exergo-environmental analysis of an integrated organic Rankine cycle for trigeneration. *Energy Convers Manag.* 2012;64:447–53. <https://doi.org/10.1016/j.enconman.2012.06.001>.
63. Hou J, Che D, Liu Y, Jiang Q. A new system of absorption heat pump vs. boiler for recovering heat and water vapor in flue gas. *Energy Procedia.* 2018;152:1266–71.
64. Ju F, Fan X, Chen Y, Ouyang H, Kuang A, Ma S, et al. Experiment and simulation study on performances of heat pump water heater using blend of R744/R290. *Energy Build.* 2018;169:148–56. <https://doi.org/10.1016/j.enbuild.2018.03.063>.
65. Nasriani HR, Jamiolahmady M, Saif T, Sánchez J. A systematic investigation into the flowback cleanup of hydraulic-fractured wells in unconventional gas plays. *Int J Coal Geol.* 2018;193:46–60. <https://doi.org/10.1016/j.coal.2018.04.012>.

**Publisher's Note** Springer Nature remains neutral with regard to jurisdictional claims in published maps and institutional affiliations.